Air-sea exchange of nitrous oxide and methane in the Arabian Sea: A simple model of the seasonal variability

Hermann W. Bange

Marine Biogeochemistry Division,Institute for Marine Research,Düsternbrooker Weg 20,24105 Kiel, Germany
[E-mail: hbange@ifm.uni-kiel.de]

With a simple box model the seasonal variability of N_2O and CH_4 were simulated in surface layers in the central and western Arabian Sea. The model was able to reproduce the N_2O measurements except for times when cold water filaments occur (i.e., during the SW monsoon). Based on the comparison of model results and measurements, it is concluded that the saturation of N_2O in the surface layer of the Arabian Sea is mainly controlled by (i) the wind-driven air-sea exchange during the SW monsoon, (ii) entrainment of N_2O from the subsurface layer, and (iii) sea surface temperature variability. However, the contribution of the factors listed above to the seasonality of the N_2O saturations is different in the selected areas. The overall good agreement of model results and the majority of N_2O measurements suggest that N_2O formation in the surface layer of the Arabian Sea is negligible. The comparison of model's results and CH_4 measurements revealed a more complex situation, partly due to considerable inconsistencies in the available CH_4 data. Thus, the situation for CH_4 remains unresolved and inconclusive.

[**Key words**: Nitrous oxide, methane, Arabian Sea, air-sea exchange, box model]

[**IPC Code:** Int. Cl.[7] C09K 3/30]

Both nitrous oxide (N_2O) and methane (CH_4) are atmospheric trace gases, which directly and indirectly, influence the present-day climate of the Earth[1]. N_2O and CH_4 are naturally produced during microbial processes such as nitrification/denitrification (N_2O) and methanogenesis (CH_4) in considerable amounts in terrestrial and oceanic environments[2,3]. Measurements of atmospheric and dissolved N_2O and CH_4 in oceanic areas are still sparse and the derived emission estimates are associated with large uncertainties mainly due to the fact that an adequate seasonal data coverage is mostly lacking[4-9]. However, due to the activities during the Arabian Sea Process Study [as part of the international Joint Global Ocean Flux Study (JGOFS) program] and other investigations, an increasing number of N_2O and CH_4 data sets for the Arabian Sea are now available[10,11]. In order to reveal the major mechanism for the observed seasonality of N_2O and CH_4 in the Arabian Sea surface layer[10,11], a model approach was chosen in which the seasonal variability of the dissolved gases is estimated from basic meteorological and hydrographical parameters. A successful modelling would allow developing tools for future monitoring of N_2O and CH_4 surface distributions and their emissions to the atmosphere in the Arabian Sea area. Using a simple box model which includes the temporal variability of air-sea exchange, the mixed surface layer depth and seawater temperature, I computed the theoretical seasonal pattern of the N_2O and CH_4 saturation in the surface layer of three selected areas in the central and western Arabian Sea and compared the model results with measurements.

Model Description

A simple box model was developed to simulate the temporal variability ($\delta C_w/\delta t$) of N_2O and CH_4 concentrations in the mixed layer (Fig. 1):

$$\delta C_w/\delta t = (\delta C_w/\delta t)_{ase} + (\delta C_w/\delta t)_{mix} \qquad \dots (1)$$

where $(\delta C_w/\delta t)_{ase}$ stands for the air-sea gas exchange across the ocean-atmosphere interface, $(\delta C_w/\delta t)_{mix}$ stands for the vertical mixing of N_2O or CH_4 into or out of the mixed layer. The present model consists of one box, the mixed surface layer, where temperature and gas concentration are homogeneously distributed. Time series of monthly seawater temperature[12], mixed layer depth[13], and wind speed[14] were used to simulate the seasonal variability of N_2O and CH_4 at three stations in the central and western Arabian Sea (Figs. 2 and 3, Table 1).
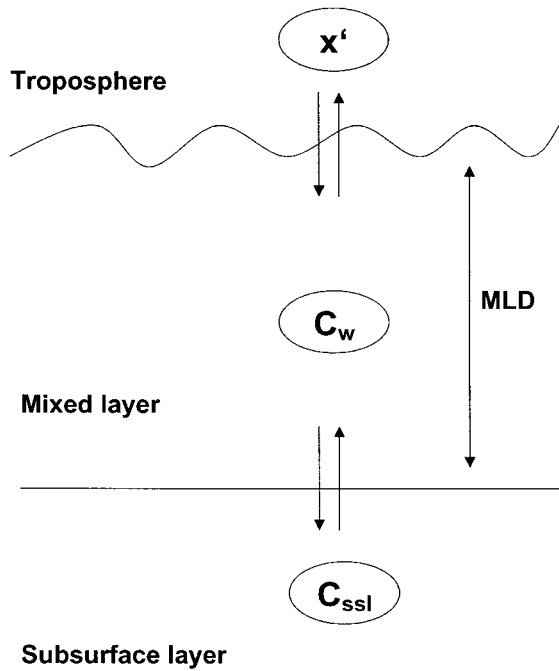
Fig. 1—Outline of the box model; C_w stands for concentration of N_2O or CH_4 in the mixed layer, C_{ssl} stands for concentration of N_2O or CH_4 in the subsurface layer, x' stands for the mole fraction of N_2O or CH_4 in the atmosphere, and MLD stands for mixed layer depth.

Table 1—Model parameters

Target areas	
SAST	09.5°–10.5° N, 64.5°–65.5° E
CAST	13.5°–15.5° N, 64.5°–65.5° E
WAST	15.5°–16.5° N, 59.5°–61.5° E
Input parameters	
Water temperature	Monthly means[a] (see Fig. 3)
Mixed layer depth	Monthly means[b] (see Fig. 3)
Wind speed	Monthly means[c] (see Fig. 3)
N_2O atmospheric mole fraction	311 ppb; 309 ppb (SW monsoon)[d]
CH_4 atmospheric mole fraction	1.8 ppm; 1.7 ppm (SW monsoon)[d]

[a] World Ocean Atlas[12].

[b] Data Set Atlas for Oceanographic Modelling Samuels & Cox[13]

[c] ECMWF Re-Analysis Project[14]

[d] During the SW monsoon the atmospheric mole fraction is lower due to fact that air masses from the southern hemisphere enter the Arabian Sea region as a consequence of the northward shift of the Intertropical Convergence Zone (ITCZ).
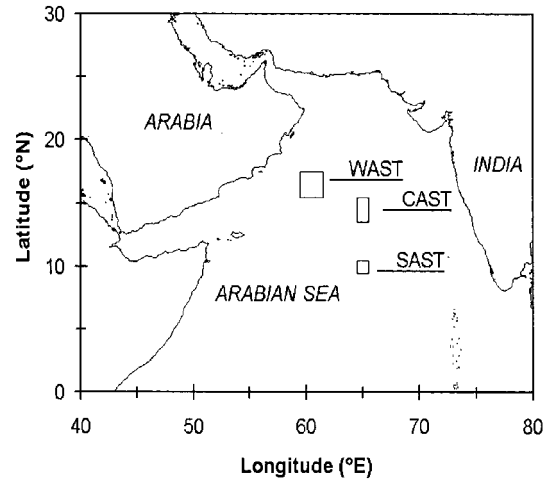

Fig. 2—Map of the Arabian Sea showing the areas WAST (Western Arabian Sea Station), CAST (Central Arabian Sea Station) and SAST (Southern Arabian Sea Station) selected for this study.

In this model, the temporal variability of gas exchange depends on the air–sea exchange flux density (F) and the mixed layer depth (MLD)[15]:

$$(\delta C_w/\delta t)_{ase} = F / MLD \qquad \ldots (2)$$

F was parameterised as :

$$F = k_w(u) \, (C_w - C_a), \qquad \ldots (3)$$

where k_w is the gas transfer coefficient as a function of wind speed (u), C_w is the N_2O seawater concentration, and C_a is the equilibrium gas concentration in seawater. C_a was calculated as :

$$C_a = \beta(SST, S) \, x', \qquad \ldots (4)$$

where x' is the atmospheric dry mole fraction and β is the Bunsen solubility, which is a function of the water temperature (SST) and salinity (S)[16,17]. To calculate k_w, the tri-linear k_w–u relationship of Liss & Merlivat[18] (LM86), the quadratic k_w–u relationship for climatological wind data of Wanninkhof[19] (W92), and the combined linear and cubic k_w–u relationship from Wanninkhof & McGillis[20] (WM99) were used. k_w was adjusted by multiplying with $(Sc/600)^{-n}$ ($n = 2/3$ for wind speeds <3.6 m s^{-1} and $n = 1/2$ for wind speeds >3.6 m s^{-1}) for LM86[18], $(Sc/660)^{-0.5}$ for W92[19] and WM99[20], where Sc is the Schmidt number for N_2O. Sc at a salinity of 35 $^o/_{oo}$ was calculated using empirical equations for the kinematic viscosity of seawater[21] and the diffusion coefficients of N_2O and CH_4 in water[22,23].
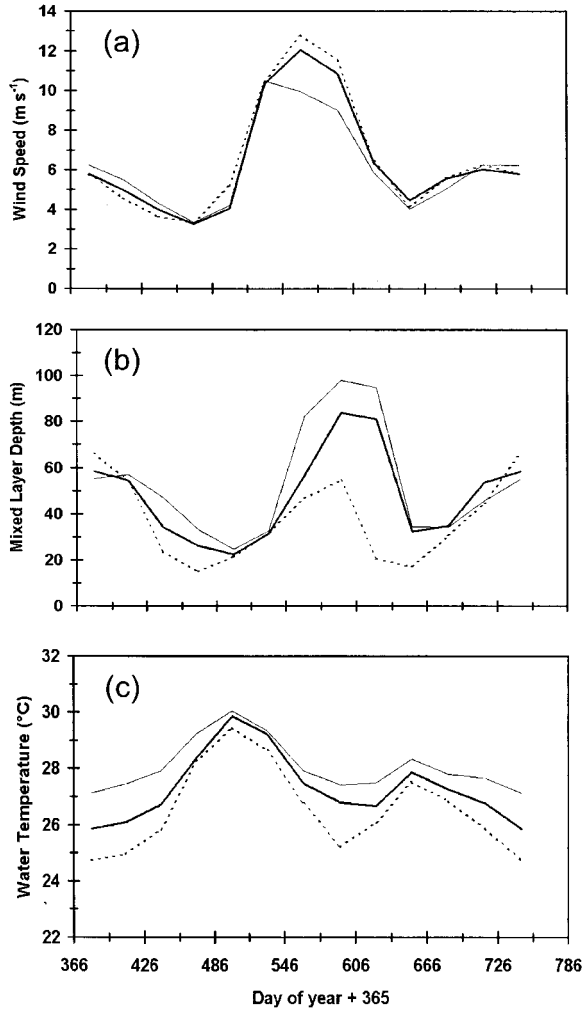
Fig. 3—Model input parameters; (a) monthly wind speeds; (b) monthly mixed layer depth; and (c) monthly water temperature for the areas WAST (dashed line), CAST (bold line) and SAST (thin line).

The gas concentration mixed into the surface layer by entrainment (ΔC_{mix}) at a given time step was computed with the approach of Peng et al.[24]:

$$\Delta C_{mix} = (C_{ssl} - C_w(t)) \, \Delta MLD \, / \, (MLD(t) + \Delta MLD) \qquad \ldots (5)$$

where C_{ssl} stands for the gas concentration in the subsurface layer (i.e., below the lower boundary of the mixed layer) and ΔMLD represents the change of the MLD at the given time step. The general shapes of N$_2$O and CH$_4$ depth profiles in the Arabian Sea suggest that surface production is not dominating their vertical distributions[25,27]. Thus, it seems reasonable to assume downward mixing to be negligible (in this case $\Delta C_w = 0$). The reported values of 8 nmol L^{-1} and

3 nmol L^{-1} were adopted for the C_{ssl} of N$_2$O and CH$_4$, respectively[25,26]. There are indications that significant spatial and seasonal variations of C_{ssl} for both N$_2$O and CH$_4$ exist[27,28]. However, seasonal and spatial variations of C_{ssl} were not introduced since appropriate time series measurements are not available. The concentration of the dissolved gases C_w at time t was calculated as follows:

$$C_w(t + \Delta t) = C_a(t + \Delta t) + \Delta C_w \qquad \ldots (6)$$

$$\Delta C_w = (F \, / \, MLD) \, \Delta t + \Delta C_{mix} \qquad \ldots (7)$$

where $C_a(t)$ is the equilibrium concentration computed with the atmospheric mixing ratio depending on the seawater temperature and salinity at the time t. The time step Δt was set to 12 hours, a value that is lower than the system's typical relaxation time, which is of the order of days or weeks depending on the wind speed and the mixed layer depth. At time $t = 0$, C_w was calculated using a prescribed saturation (Sat in %, i.e., 100% = equilibrium):

$$C_w(0) = C_a(0) \, Sat \, / \, 100 \qquad \ldots (8)$$

The results of the model computations are presented as saturation $Sat(t)$ of at time t in the mixed surface layer:

$$Sat(t) = 100 C_w(t) \, / \, C_a(t) \, [\%] \qquad \ldots (9)$$

The model results become stable within the first model year, thus results from the second model year are shown (days 366–745).

Model input parameters are listed in Table 1. Model results were compared to saturation data from the data sets for N$_2$O[29-32] as well as for CH$_4$[26,32,33].

Results and Discussion

Nitrous oxide (N$_2$O)

Figure 4 shows the results of the N$_2$O model runs for the SAST (Southern Arabian Sea Station at 10°N 65°E), CAST (Central Arabian Sea Station at 14.5°N 65°E) and WAST (Western Arabian Sea Station at 16.3°N 60.5°E) areas. Generally, the model results show enhanced N$_2$O saturations during the first intermonsoon period from March to late May with maximum values at the end of April (around model day 486). This is caused by the seasonal increase of the SST, which causes higher N$_2$O saturation because of lower solubility and the fact that the variation in SST is faster than the equilibration time of the air-sea
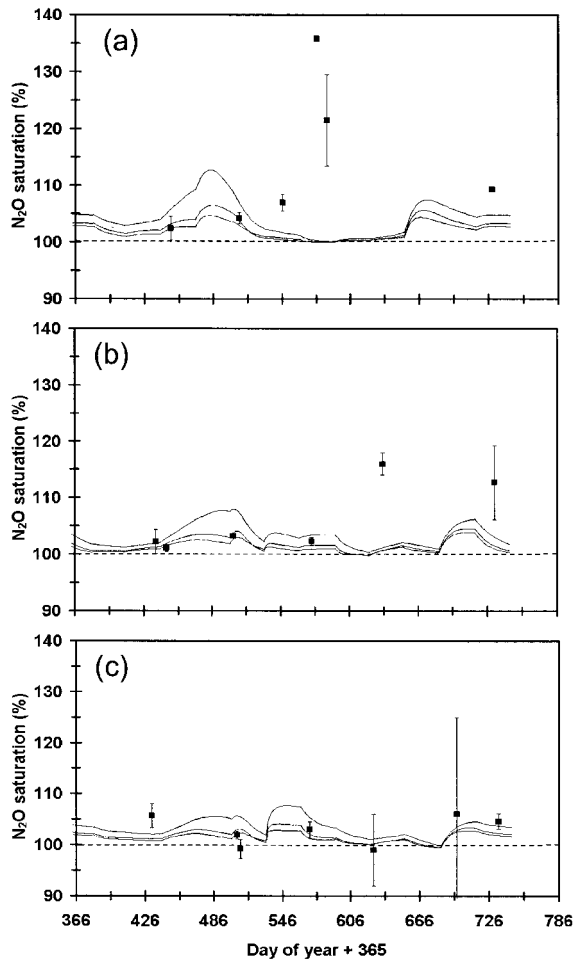
Fig. 4—Results of the N$_2$O model; (a) WAST, (b) CAST and (c) SAST. Measurements are given as mean values with standard deviation (when available). Three different air-sea exchange models were applied (see text for details). The air-sea exchange models of Liss & Merlivat[18] and Wanninkhof[19] envelop the range of model results.

exchange. During the southwest (SW) monsoon (late May–September, model days 510–638), N$_2$O saturations are driven by both the high monsoonal wind speeds and the seasonal deepening of the *MLD*. However the effects are counteracting. High wind speeds lead to high emissions and subsequent depletion of N$_2$O in the mixed layer, whereas deepening of the mixed layer leads to an entrainment of N$_2$O from the subsurface layer. Since the mixed layer deepening is most pronounced at SAST (Fig. 2), the effect of entrainment is most pronounced at SAST, but almost not visible at station WAST. The winter deepening of the *MLD* during the end of the secondintermonsoon and the northeast (NE) monsoon from mid of October to January (model days 653–745) leads to a third period of enhanced saturations
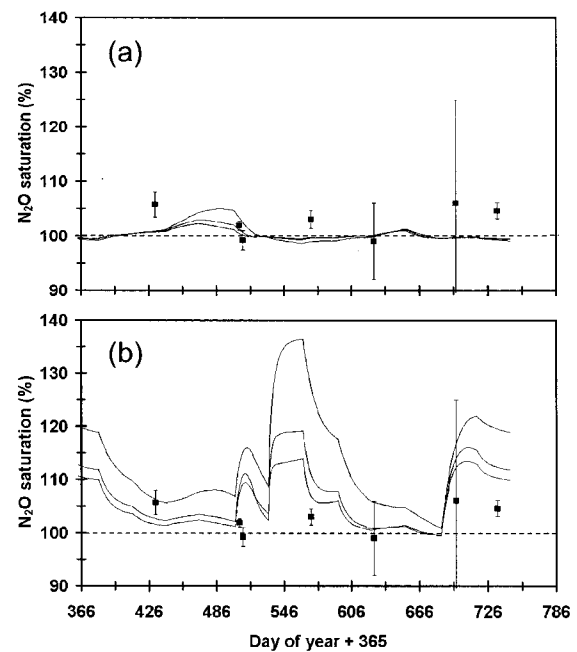

Fig. 5—N$_2$O model results for station SAST; (a) without entrainment (C_{ssl} = 0 nmol L^{-1}), (b) with entrainment (C_{ssl} = 16 nmol L^{-1}). Three different air-sea exchange models were applied (see text for details). The air-sea exchange models of Liss & Merlivat[18] and Wanninkhof[19] envelop the range of model results.

because of the entrainment of N$_2$O from the subsurface layer.

In order to check the model sensitivity for the choice of C$_{ssl}$, we performed model runs for station SAST with extreme values for C_{ssl} (0 and 16 nmol L^{-1}) (Fig. 5). The incorporation of moderate entrainment (C_{ssl} = 8 nmol L^{-1}, Fig. 4c) brings the model results at station SAST (and at station CAST, sensitivity runs not shown) into a good agreement with the measurements, indicating that the basic assumption of C_{ssl} = 8 nmol L^{-1} is reasonable.

For comparison, N$_2$O saturations based on measurements are shown in Fig. 4. There is a good agreement between the measurements and model results for SAST and partly for stations CAST and WAST as well. At station WAST, maximum N$_2$O saturations of up to 135% have been reported for the SW monsoon period, however, these values are not matched by the model results. This discrepancy is due to the fact that the WAST area is influenced by cold water filaments which originate from upwelling centres at the coast of the Arabian peninsula[34]. Arabian Sea filaments typically show enhanced N$_2$O concentrations[30,35]. Filaments might cause the mismatch of model results and measurements at CAST during the late SW monsoon as well. However,

this result is not surprising, since advective processes are not parameterised in the model. Lal & Patra[36] reported surface N$_2$O saturations for the NE and SW monsoons and for the intermonsoon (April–May) at stations in the proximity of SAST and CAST. Their values lie in the range from 110% to 152% with highest values during the NE monsoon in February/March (136% at stations close to SAST and 152% at stations close to CAST). It appears that the present model when extended to their stations would not represent the monsoon data by Lal & Patra[36]. The reason for the apparent discrepancy might be due to strong advective processes during the SW monsoon together with an unusual deepening of the mixed layer during the NE monsoon.

Methane (CH$_4$)

Figure 6 shows the modelled CH$_4$ saturations for the stations SAST, CAST and WAST. The general shape of the model results is similar to the N$_2$O model results (see previous section). In contrast to the N$_2$O model, a comparison of CH$_4$ model results and measurements reveal significant discrepancies. At SAST the model generally underestimates the observed CH$_4$ saturations, whereas at CAST and WAST some of the measurements are in very good agreement with the model results. Therefore, a general conclusion is difficult to draw. On the one hand, one might argue that a missing CH$_4$ formation in the surface layer might be the reason for a general underestimation of the model. On the other hand, the very good agreement of some measurements and model results at CAST and WAST does not imply a missing CH$_4$ source. Additionally, some of the discrepancies arise because there is considerable inconsistency in the CH$_4$ measurements. For example, at CAST a difference in the CH$_4$ observations of up to 40% CH$_4$ saturation was noted, based on two independent observations on the same day and the same year. Similar inconsistencies also occur in the data set of the WAST area.

Conclusion

With a simple box model the seasonal variability of the saturations of N$_2$O and CH$_4$ in surface layers of three areas in the central and western Arabian Sea have been simulated. The model was able to reproduce the N$_2$O measurements except for times when cold water filaments occur (i.e., at WAST and CAST during the SW monsoon). Based on the
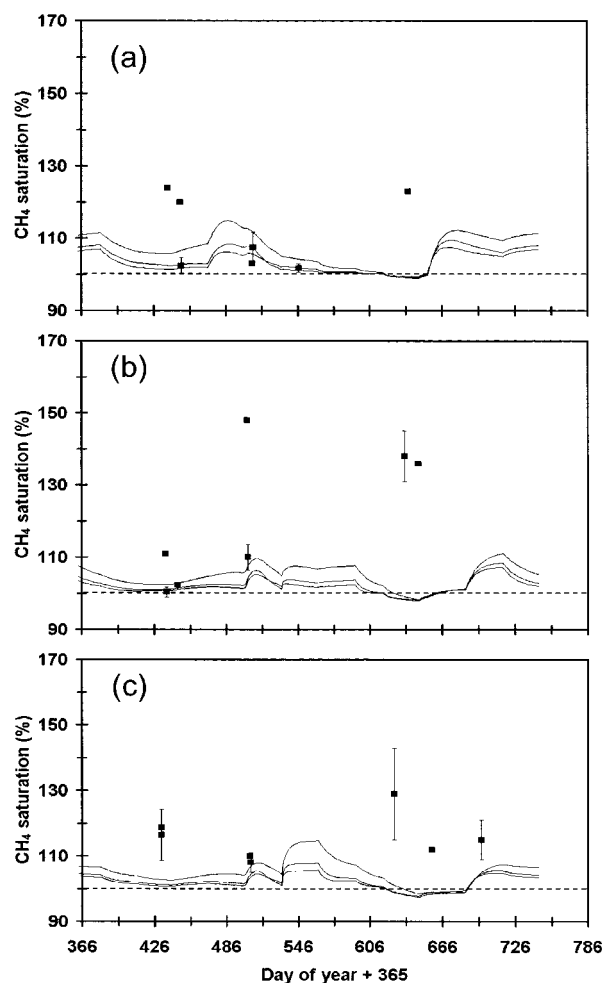

Fig. 6—Results of the CH$_4$ model; (a) WAST, (b) CAST and (c) SAST. Measurements are given as mean values with standard deviation (when available). Three different air-sea exchange models were applied (see text for details). The air-sea exchange models of Liss & Merlivat[18] and Wanninkhof[19] envelop the range of model results.

comparison of model results and measurements, it is concluded that the saturation of N$_2$O in the surface layer of the Arabian Sea is mainly controlled by (i) the wind-driven air-sea exchange during the SW monsoon, (ii) entrainment of N$_2$O from the subsurface layer, and (iii) SST variability. However, the contribution by the factors listed above to the seasonality of the N$_2$O saturations is different. For example, N$_2$O saturations at CAST during the non-monsoon season are mainly determined by the seasonal variability of the SST, whereas at the southernmost area (SAST), the entrainment of N$_2$O results in maximum N$_2$O saturations during the SW monsoon season. It has been suggested that N$_2$O might be produced in the ocean surface layer of the

subtropical Pacific Ocean[37] and the Caribbean Sea[38]. However, the overall good agreement of model results and measurements suggests that N_2O formation in the surface layer of the Arabian Sea is negligible. This is in agreement with the results by Naqvi & Noronha[39].

The situation for CH_4 appears to be more complex. The comparison of model results and CH_4 measurements at SAST revealed a considerable underestimation by the model, possibly indicating an *in-situ* source of CH_4 in the surface layer as suggested by various authors[40-42]. However, the results for stations CAST and WAST are not in line with this result, partly due to the considerable inconsistency of the available CH_4 measurements. Thus, the situation for CH_4 remains unresolved and no final conclusion can be drawn for CH_4.

Acknowledgement

References

1   Prather M, Ehhalt D, Dentener F, Derwent R, Dlugokencky E, Holland E, Isaksen I, Katima J, Kirchhoff V, Matson P, Midgley P & Wang M, Atmospheric chemistry and greenhouse gases, in: *Climate Change 2001: The Scientific Basis Contribution of Working Group I to the Third Assessment Report of the Intergovernmental Panel on Climate Change*, edited by JT Houghton, Ding, Y, Griggs, DJ, Noguer, M, Van der Linden, P J, Dai, X, Maskell, K & Johnson, C A, (Cambridge University Press, Cambridge), 2001, pp. 239–287.

2   Cicerone R J & Oremland R S, Biogeochemical aspects of atmospheric methane, *Global Biogeochem Cycles,* 2 (1988) 299–327.

3   Codispoti L A, Brandes J A, Christensen J P, Devol A H, Naqvi S W A, Paerl H W & Yoshinari T, The oceanic fixed nitrogen and nitrous oxide budgets: Moving targets as we enter the anthropocene? *Scientia Marina,* 65 (2001) 85–105.

4   Bange H W, Rapsomanikis S & Andreae M O, Nitrous oxide in coastal waters, *Global Biogeochem Cycles,* 10 (1996) 197–207.

5   Nevison C D, Weiss R F & Erickson III D J, Global oceanic emissions of nitrous oxide, *J Geophys Res,* 100 (1995) 15,809–15,820.

6   Suntharalingam P & Sarmiento J L, Factors governing the oceanic nitrous oxide distribution: Simulations with an ocean general circulation model, *Global Biogeochem Cycles,* 14 (2000) 429–454.

7   Seitzinger S P, Kroeze C & Styles R V, Global distribution of N_2O emissions from aquatic systems: Natural emissions and anthropogenic effects, *Chemosphere: Global Change Sci,* 2 (2000) 267–279.

8   Bange H W, Bartell U H, Rapsomanikis S & Andreae M O, Methane in the Baltic and North Seas and a reassessment of the marine emissions of methane, *Global Biogeochem Cycles,* 8 (1994) 465–480.

9   Bates T S, Kelly K C, Johnson J E & Gammon R H, A reevaluation of the open ocean source of methane to the atmosphere, *J Geophys Res,* 101 (1996) 6953–6961.

10 Bange H W, Andreae M O, Lal S, Law C S, Naqvi S W A, Patra P K, Rixen T & Upstill-Goddard R C, Nitrous oxide emissions from the Arabian Sea: A synthesis, *Atmos Chem Phys,* 1 (2001) 61–71.

11 Naqvi S W A, Bange H W, Gibb S W, Goyet C, Hatton A D & Upstill-Goddard R C, Biogeochemical ocean-atmosphere transfers in the Arabian Sea, *Progr Oceanogr,* 2004 (submitted).

12 Conkright M, Levitus S & Boyer T P, NOAA Atlas NESDIS 1, World Ocean Atlas 1994 (National Environmental Satellite, Data, and Information Service, National Oceanic and Atmospheric Administration, US Department of Commerce, Washington DC) 1994.

13 Samuels B L, & Cox M, Data set atlas for oceanographic modeling, *Ocean Modeling,* 75 (1987) 1–3.

14 Gibson J K, Kållberg P, Uppala S, Hernandez A, Nomura A & Serrano E, ECMWF Re-Analysis Project Report Series 1 ERA description, (European Centre for Medium-Range Weather Forecasts, Reading, UK), 1997, pp. 72.

15 Louanchi F, Metzl N & Poisson A, Modelling the monthly sea surface-CO_2 fields in the Indian Ocean, *Mar Chem,* 55 (1996) 265–279.

16 Weiss R F & Price B A Nitrous oxide solubility in water and seawater, *Mar Chem,* 8 (1980) 347–359.

17 Wiesenburg D A & Guinasso Jr N L, Equilibrium solubilities of methane, carbon monoxide, hydrogen in water and seawater, *J Chem Eng Data,* 24 (1979) 356–360.

18 Liss P S & Merlivat L, "Air-sea exchange rates: Introduction and synthesis", in: *The role of air-sea exchange in geochemical cycling,* edited by P Buat-Ménard, (D Reidel Publishing Company, Dordrecht) 1986, pp.113–127.

19 Wanninkhof R, Relationship between wind speed and gas exchange over the ocean, *J Geophys Res,* 97 (1992) 7373–7382.

20 Wanninkhof R & McGillis W R A cubic relationship between air-sea gas CO_2 exchange and wind speed, *Geophys Res Lett,* 26 (1999) 1889–1892.

21 Siedler G & Peters H, Properties of sea water, in: *Oceanography, Landolt-Börnstein New Series Vol V/3a,* edited by J Sündermann, (Springer Verlag, Berlin) 1986, pp. 233–264.

22 Broecker W S & Peng T H, Gas exchange rates between air and sea, *Tellus,* 26 (1974) 21–35.

23 Jähne B, Heinz G & Dietrich W, Measurements of the diffusion coefficients of sparingly soluble gases in water, *J Geophys Res,* 92 (1987) 10,767–10,776.

24 Peng T H, Takahashi T, Broecker W S & Olafsson J, Seasonal variability of carbon dioxide, nutrients and oxygen

in the North Atlantic surface water: Observations and a model, *Tellus*, 39B (1987) 439–458.

25 Bange H W, Rapsomanikis S & Andreae M O, Nitrous oxide cycling in the Arabian Sea, *J Geophys Res*, 106 (2001) 1053–1065.

26 Delling N, *Volatile hydrocarbons in the Arabian Sea – Distribution, formation and budgeting* [*Leichtflüchtige Kohlenwasserstoffe im Arabischen Meer – Verteilung, Genese und Bilanzierung*], Ph.D. thesis, University of Hamburg, Germany, 2002.

27 Patra P K, Lal S, Venkataramani S, Gauns M & Sarma V V S S, Seasonal variability in distribution and fluxes of methane in the Arabian Sea, *J Geophys Res*, 103 (1998) 1167–1176.

28 Patra P K, Lal S, Venkataramani S, De Sousa S N, Sarma V V S S & Sardesai S, Seasonal and spatial variability in N$_2$O distribution in the Arabian Sea, *Deep-Sea Res I*, 46 (1999) 529–543.

29 Bange H W, Rixen T, Johansen A M, Siefert R L, Ramesh R, Ittekkot V, Hoffmann, M R & Andreae, M O, A revised nitrogen budget for the Arabian Sea, *Global Biogeochem Cycles*, 14 (2000) 1283–1297.

30 Bange H W, Rapsomanikis S & Andreae M O, Nitrous oxide emissions from the Arabian Sea, *Geophys Res Lett*, 23 (1996) 3175–3178.

31 Weiss R F, Van Woy F A & Salameh P K, *Surface water and atmospheric carbon dioxide and nitrous oxide observations by shipboard automated gas chromatography: Results from expeditions between 1977 and 1990*, Report no SIO 92-11, ORNL/CDIAC-59, NDP-044 (Carbon Dioxide Information Analysis Center, Oak Ridge National Laboratory, Oak Ridge, Tennessee, USA) 1992.

32 Upstill-Goddard R C, Barnes J & Owens N J P, Nitrous oxide and methane during the 1994 SW monsoon in the Arabian Sea/northwestern Indian Ocean, *J Geophys Res*, 104 (1999) 30,067–30,084.

33 Bange H W, Ramesh R, Rapsomanikis S & Andreae M O, Methane in the surface waters of the Arabian Sea, *Geophys Res Lett*, 25 (1998) 3547–3550.

34 Lee C M, Jones B H, Brink K H & Fischer A S, The upper-ocean response to monsoonal forcing in the Arabian Sea: Seasonal and spatial variability, *Deep-Sea Res II*, 47 (2000) 1177–1226.

35 Lendt R, Hupe A, Ittekkot V, Bange H W, Andreae M O, Thomas H, Al Habsi S & Rapsomanikis S, Greenhouse gases in cold water filaments in the Arabian Sea during the southwest monsoon, *Naturwissenschaften*, 86 (1999) 489–491.

36 Lal S & Patra P K, Variabilities in the fluxes and annual emissions of nitrous oxide from the Arabian Sea, *Global Biogeochem Cycles*, 12 (1998) 321–327.

37 Dore J E & Karl D M, Nitrification in the euphotic zone as a source for nitrite, nitrate, and nitrous oxide at station ALOHA, *Limnol Oceanogr*, 41 (1996) 1619–1628.

38 Morell J M, Capella J, Mercado A, Bauzá J & Corredor J E, Nitrous oxide fluxes in Caribbean and tropical Atlantic waters: Evidence for near surface production, *Mar Chem*, 74 (2001) 131–143.

39 Naqvi S W A & Noronha R J, Nitrous oxide in the Arabian Sea, *Deep-Sea Res*, 38 (1991) 871–890.

40 Karl D M & Tilbrook B D, Production and transport of methane in oceanic particulate organic matter, *Nature*, 368 (1994) 732–734.

41 De Angelis M A & Lee C, Methane production during zooplankton grazing on marine phytoplankton, *Limnol Oceanogr*, 39 (1994) 1298–1308.

42 Holmes E, Sansone F J, Rust T M & Popp. B N, Methane production, consumption, and air-sea exchange in the open ocean: An evaluation based on carbon isotopic ratios, *Global Biogeochem Cycles*, 14 (2000) 1–10.